Electronic Supplementary Information (ESI) for Chemical Communications. This journal is (c) The Royal Society of Chemistry 2022.

Electronic Supplementary Information (ESI)

Rational Engineering VS_4 nanorod array on rose-shaped VS_2 nanosheets for high-performance aluminum-ion batteries

Yan Wang,[a] Zihan Shen,[b] Xirong Lin,[c] Qian Ding,[a] Xiaofei Huang,[a] Tianli Han,[*a] Huigang Zhang,[*b,d] and Jinyun Liu[*a]

Experimental section

Preparation of rose-shaped VS_2 microspheres: All chemicals were used directly without further treatment. The VS_2 microspheres were prepared by using a simple hydrothermal method. In a water bath, 4 mmol ammonium metavanadate (NH_4VO_3) was dispersed in 30 mL ultra-pure water, 25 mmol thioacetamide (TAA) and 4 mL concentrated ammonia ($NH_3 \cdot H_2O$) were successively added. The mixed solution was stirred vigorously for 1 h, then transferred into a reaction kettle. After reaction at 180 °C for 8 h, the sample was washed three times with pure water and alcohol, then dried in an oven.

Preparation of VS_2@VS_4 composite: Under the condition of water bath at 80 °C, 3 mmol NH_4VO_3 and 0.5 g polyether F127 were dispersed in 30 mL ultrapure water to obtain solution A. Under the same conditions, 50 mmol TAA and 0.2 g VS_2 were dispersed in 30 mL ethylene glycol (EG) to obtain solution B, which was added into A drop by drop and stirred for 0.5 h.

The mixed solution was transferred to a reaction kettle and reacted at 160 ºC for 12 h. After that, the sample was collected and washed.

Characterization: The phrase of the sample was determined by using an X-ray diffractometer (XRD, SMART APEX II Brook, copper target, Kα X-ray wavelength=1.5418 Å). The morphology was observed by field emission scanning electron microscope (SEM), Hitachi S-8100, and transmission electron microscope (TEM, HT-7700, TecnaiG220S-Twin). A high-resolution TEM (HRTEM) was used to observe the lattice fringes. Energy dispersive X-ray spectroscopy (EDX) was employed for elemental mapping and studying the elemental distribution. X-ray photoelectron spectroscopy (XPS, EscalAB250) and Raman spectroscopy (Renishaw in Via) were used for characterization. Before measuring the specific surface area, the sample was degassed in a vacuum at 120 ºC for 6 h to remove the adsorbed water and surface impurities. The physical adsorption isotherms were measured in nitrogen at 77 K using an ASAP Micromeritics Tristar 2460 instrument.

First-principle computation: During DFT modeling, a plane wave basis set with an energy cutoff of 500 eV was adopted and the Brillouin zone integration was conducted on a 2×2×2 Monkhorst–Pack k-point mesh. The cell parameter was 16.04×16.04×12.93 Å for VS_2@VS_4 heterostructures; and all atoms were fully relaxed during the geometry optimization.

Electrochemical tests: The VS_2@VS_4 composite (70 wt%) and conductive carbon black (20 wt%) were mixed, grounded for 30 min, then polyvinylidene fluoride (PVDF, 10 wt%) and Nmethylpyrrolidone (NMP, 6.54 wt%) were added. It is noted that we used the PVDF on the basis of some reports [1,2]; however, the compatibility of PVDF in some electrolyte systems would be not good enough, which inspired a potential research direction in future. The slurry was coated on a carbon paper, dried in a vacuum oven at 80 ºC for 24 h, and cut into 12 mm-diameter discs. The water and oxygen values were less than 0.01 ppm in a glove box (MIKROUNA, Super1220/750/900), which was filled with argon gas. In the 2032-typed coin cell system, a molybdenum disc with a diameter of 20 mm and a thickness of 0.02 mm was added to prevent the corrosion of the electrolyte on the cell shell before dropping the electrolyte. The counter electrode was aluminum foil; and the diaphragm was glass fiber. The electrolyte was $AlCl_3$:[EMIm]Cl=1.3:1 with a n electrolyte volume/mass of 60 μL mg^{-1}. In the voltage range of 0.01-2.0 V, the cycling and rate-performance were explored by using a galvanostatic method charge-discharge mode. *In-situ* reaction resistance was measured by constant-current intermittent titration (GITT). Cyclic voltammetry (CV) was measured on an electrochemical workstation (CHI660e). For the tests at different temperatures, the batteries were put in a temperature-controlled chamber with a determined temperature. Prolonged lines were used to connect the tester (NEWARE, CT-4008) and batteries. Before starting each test, the batteries were putting in the low temperature chamber overnight.

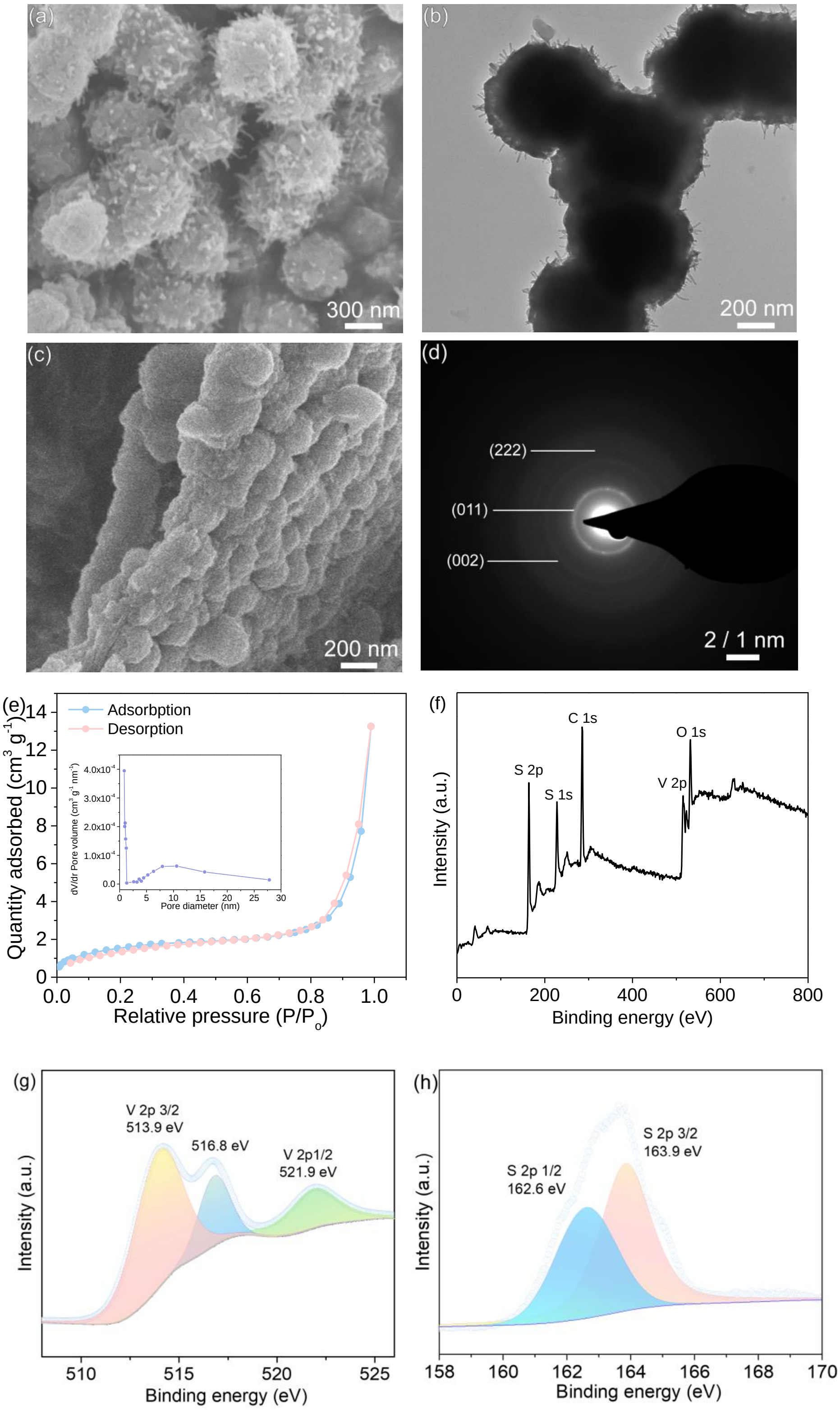

Fig. S1 (a) SEM and (b) TEM images of VS_4. (c) SEM images and (d) SAED pattern of $VS_2@VS_4$. (e) Adsorption-desorption isothermal and pore-size distribution of $VS_2@VS_4$. XPS spectra: (f) survey spectrum, (g) V 2p and (h) S 2p of $VS_2@VS_4$.

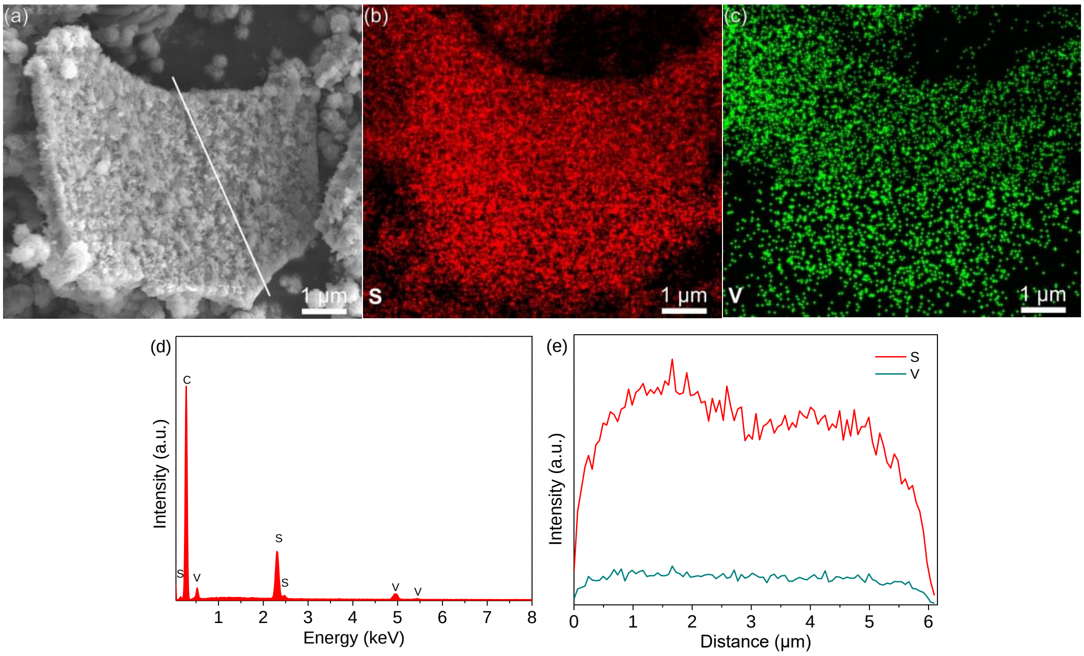

Fig. S2 (a) SEM images, (b,c) S and V elemental mapping, (d) EDS spectrum, and (e) line-scanning curves of $VS_2@VS_4$.

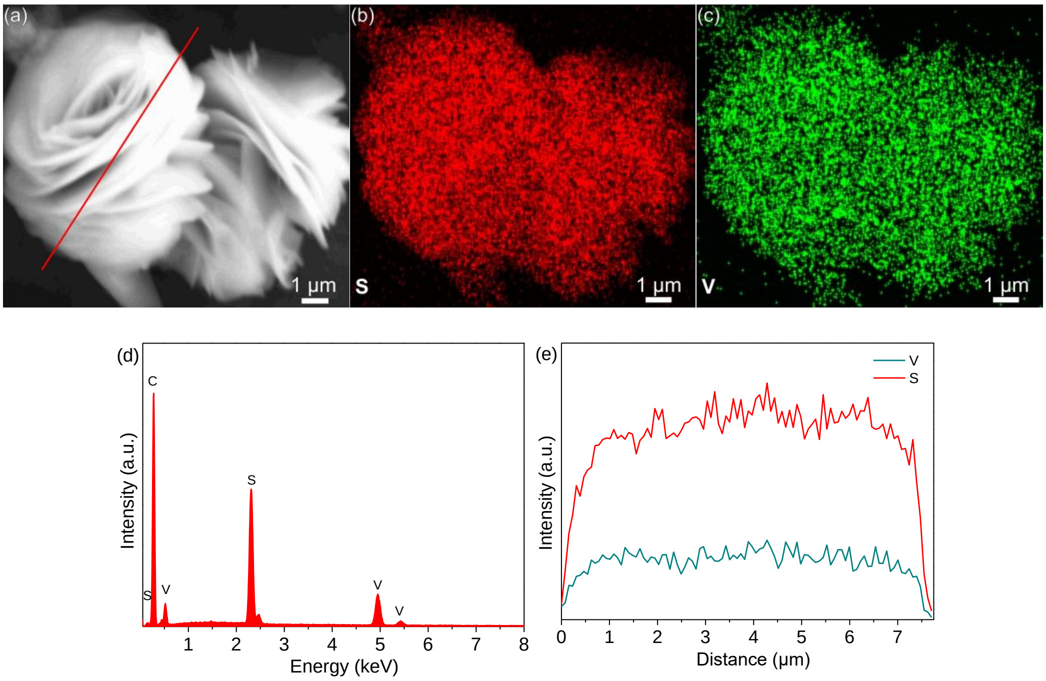

Fig. S3 (a) SEM image, (b,c) S and V elemental mapping, (d) EDS spectrum, and (e) line-scanning curves of VS_2.

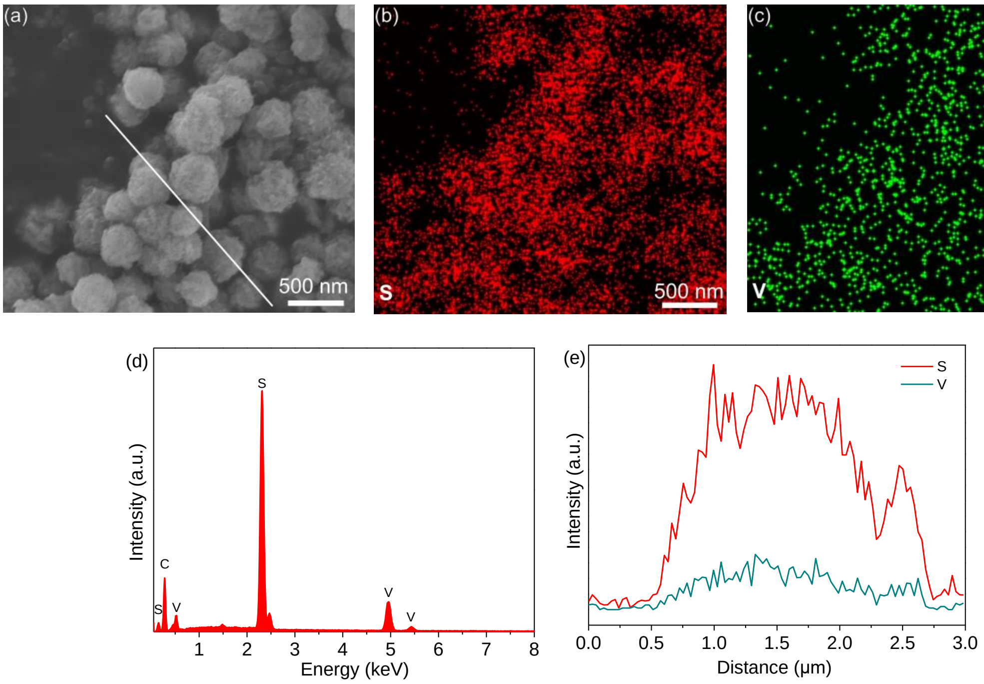

Fig. S4 (a) SEM image, (b,c) S and V elemental mapping, (d) EDS spectrum, and (e) line-scanning curves of VS_4.

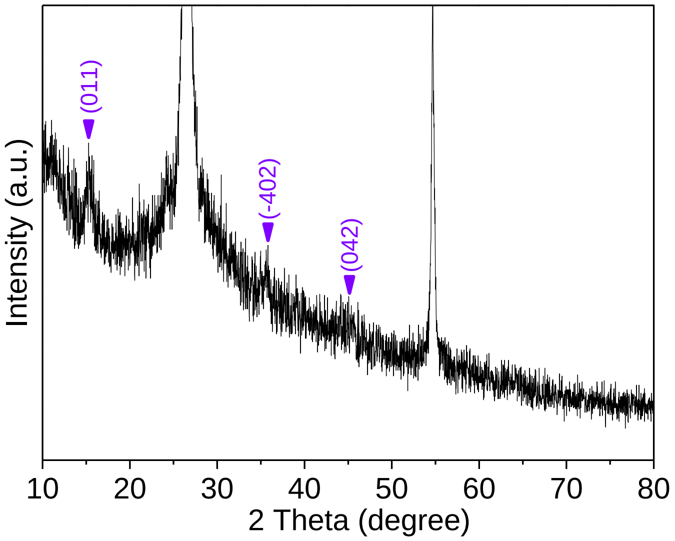

Fig. S5 XRD patterns of VS_2@VS_4 after 100 cycles at 0.3 A g^{-1}.

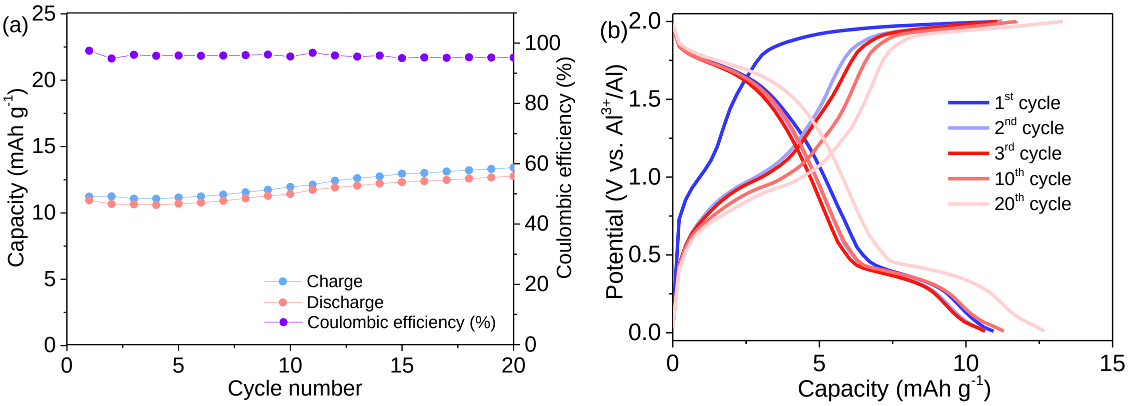

Fig. S6 (a) Cycling performance and (b) charge-discharge curves of pure carbon paper cycling at 0.013 A g^{-1}.

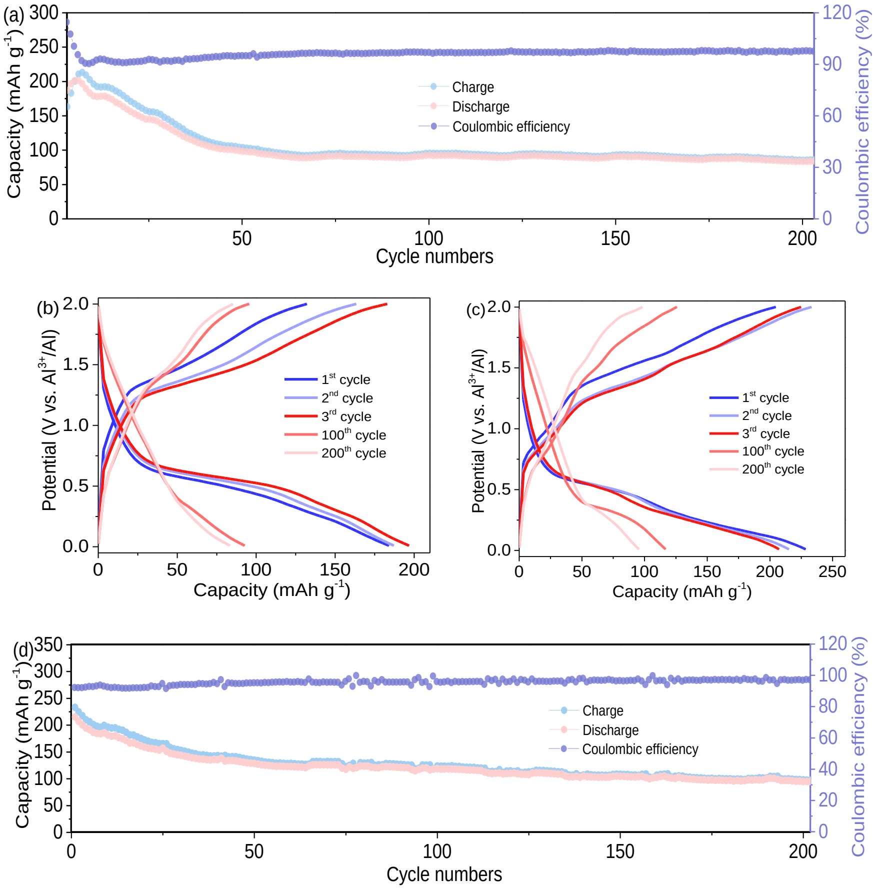

Fig. S7 (a) Cycling performance and (b) charge-discharge profiles of VS$_2$@VS$_4$ with a loading of 2.61 mg cm^{-2} at 0.3 A g^{-1}. (c) Cycling performance and (b) charge-discharge curves of VS$_2$ with a loading of 2.2 mg cm^{-2} at 0.2 A g^{-1}.

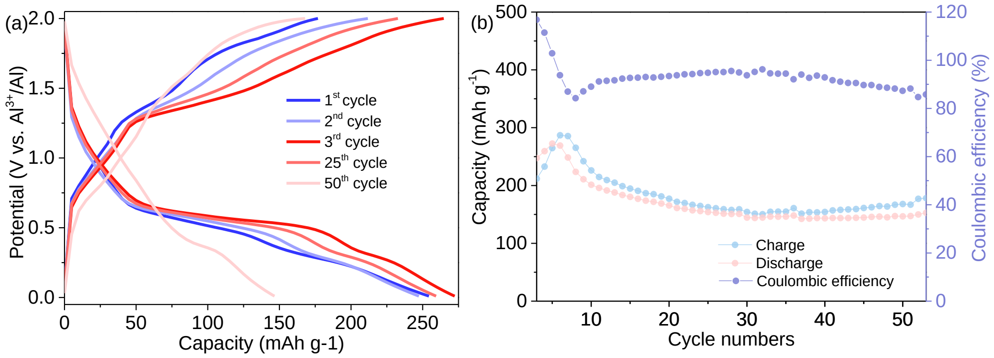

Fig. S8 (a) Charge-discharge profiles and (b) cycling performance of VS_4 at 0.3 A g^{-1}.

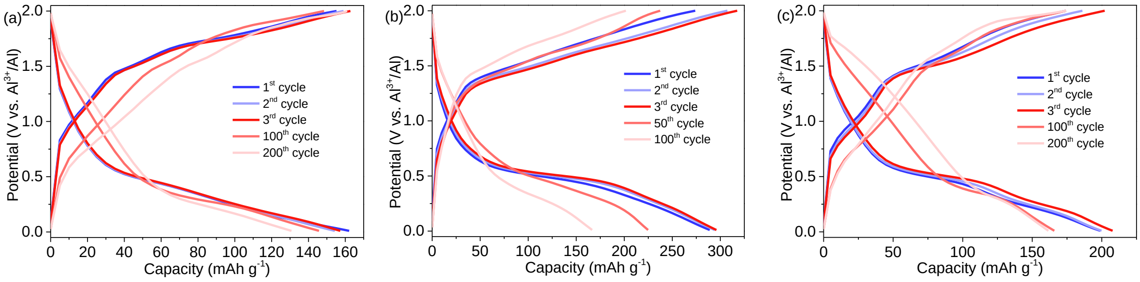

Fig. S9 Charge-discharge profiles of (a)VS_2, (b)VS_4, (c)VS_2@VS_4 at –10 °C.

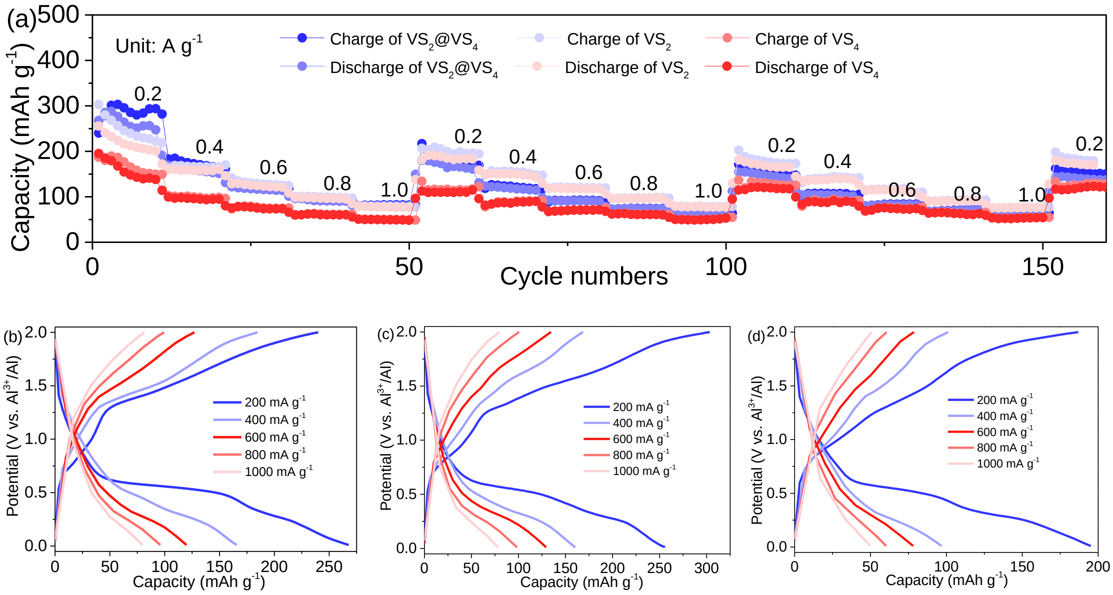

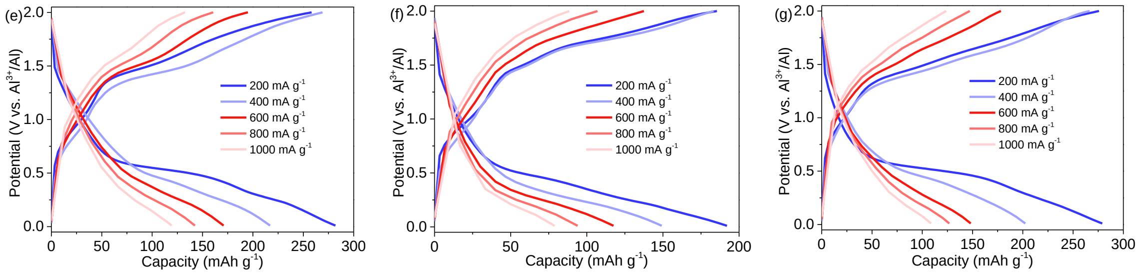

Fig. S10 (a) Rate-performance of VS_2, VS_4 and VS_2@VS_4 at room temperature. Charge-discharge profiles of (b) VS_2@VS_4, (c) VS_2 and (d) VS_4. Charge-discharge profiles of (e) VS_2@VS_4, (f) VS_2 and (g) VS_4 at –10 °C.

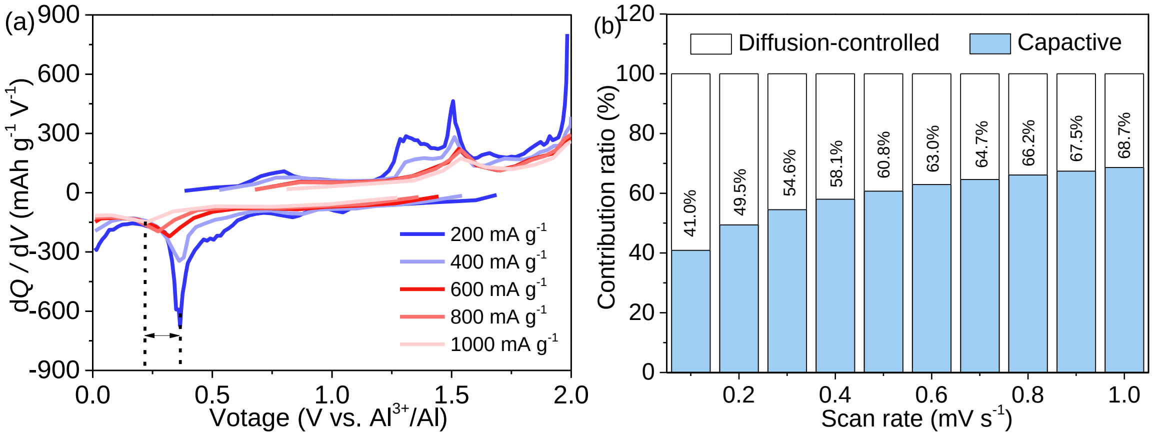

Fig. S11 (a) Differential specific capacity versus voltage plots at various rates. (b) Contribution ratio of capacitive and diffusion-control processes.

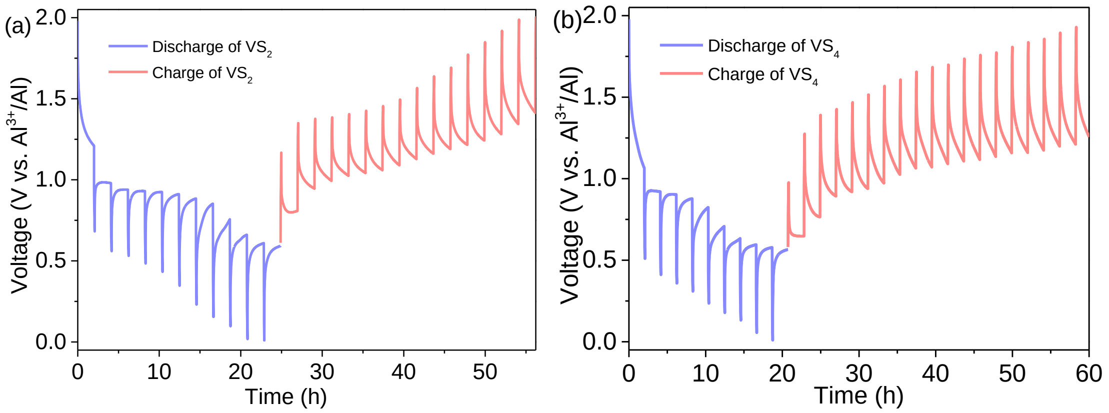

Fig. S12 GITT time-potential distributions of (a) VS_2, and (b) VS_4.

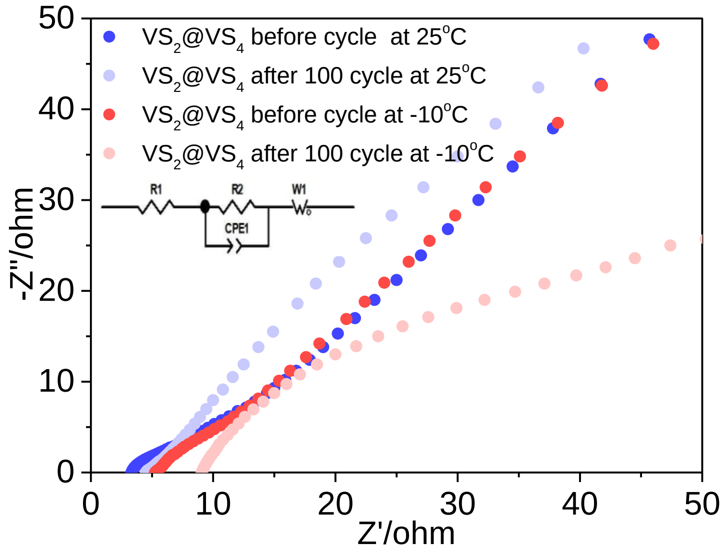

Fig. S13 EIS spectrum of VS$_2$@VS$_4$ before and after cycling under 25 ºC and –10 ºC.

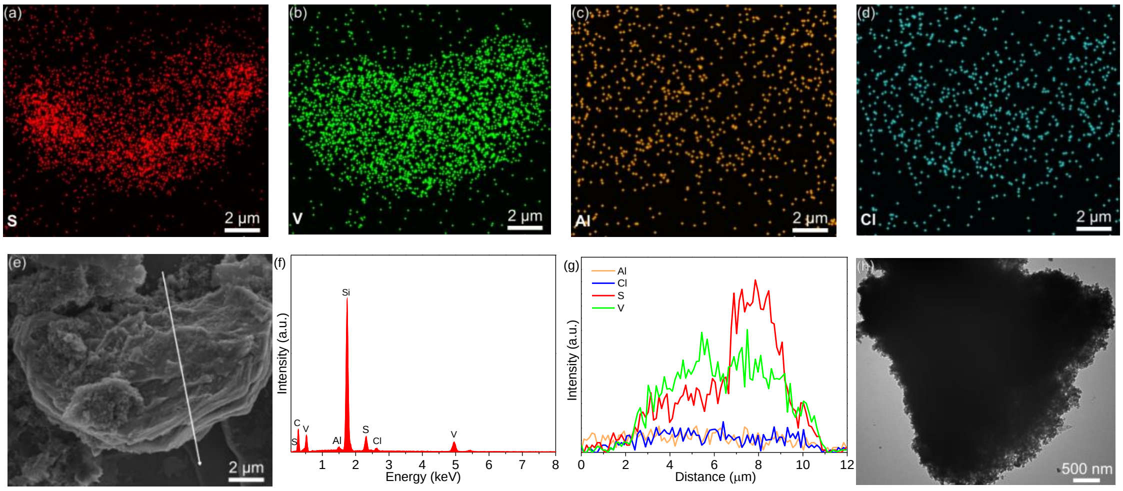

Fig. S14 (a-d) Elemental mapping of S, V, Al and Cl, (e) SEM image, (f) EDS spectrum, (g) line-scanning curves, and (h) TEM image of VS$_2$@VS$_4$ after 100 cycles at 0.3 A g^{-1}.

Table S1. Comparison on the cycling performance of some cathodes.

Composite	Current density ($A\ g^{-1}$)	Cycle number	Capacity ($mAh\ g^{-1}$)	Ref.
δ-MnO_2 nanofibers	0.1	100	37	3
Nanosphere-rod-like Co_3O_4	0.2	100	122.1	4
VOCl	0.05	100	41.5	5
Graphitized soft carbon	0.5	1000	77.7	6
Hexagonal NiS nanobelts	0.2	100	100	7
SnSe	0.3	100	107	8
MoS_2	0.04	100	66.7	9
MoO_2@Ni	0.1	100	90	10
Cu-Al	0.1	1000	82.3	11
$Cu_{2-x}Se$	0.2	100	100	12
Co-P	0.2	400	85.1	13
Hierarchical VS_2@VS_4	0.3	500	116.5	This work

Reference

1 D. Y. Wang, C.Y. Wei, M. C. Lin, C. J. Pan, H. L. Chou, H. A. Chen,M. Gong, Y. Wu, C.Yuan, M. Angell, Y. J. Hsieh, Y. H. Chen, C. Y. Wen, C. W. Chen, B. J. Hwang, C. C. Chen and H. Dai, Advanced rechargeable aluminium ion battery with a high-quality natural graphite cathode, *Nat. Commun.*, 2017, 8, 14283.

2 D. J. Yoo, M. Heeney, F. Glöcklhofer and J. W. Choi, Tetradiketone macrocycle for divalent aluminium ion batteries, *Nat. Commun.*, 2021, 12, 2386.

3 P. Almodovar, D. A. Giraldo, J. Chancon, I. Alvarez-Serrano and M. L. Lopez, *ChemElectroChem*, 2020, 7, 2102-2106.

4 J. Liu, Z. Li, X. Huo and J. Li, *J. Power Sources*, 2019, 422, 49-56.

5 Q. Yan, Y. Shen, Y. Miao, M. Wang, M. Yang and X. Zhao, *J. Alloys Compd.*, 2019, 806, 1109-1115.

6 J. Qiao, H. Zhou, Z. Liu, H. Wen and J. Yang, *Ionics*, 2019, 25, 1235-1242.

7 Z. Yu, Z. Kang, Z. Hu, J. Lu, Z. Zhou and S. Jiao, *Chem. Commun.*, 2016, 52, 10427.

8 Y. Zhang, B. Zhang, J. Li, J. Liu, X. Huo and F. Kang, *Chem. Eng. J.*, 2021,403, 126377.

9 Z. Li, B. Niu, J. Liu, J. Li and F. Kang, *ACS Appl. Mater. Interfaces*, 2018, 10, 9451-9459.

10 J. Wei, W. Chen, D. Chen and K. Yang, J. Electrochem. Soc., 2017, 164, A2304-A2309.

11 H. Jiao, S. Jiao, W. L. Song, H. Chen, M. Wang, J. Tu and D. Fang, *J. Electrochem. Soc.*, 2019, 166, A3539-A3545.

12 J. Jiang, H. Li, T. Fu, B. J. Hwang, X. Li and J. Zhao, *ACS Appl. Mater. Interfaces*, 2018, 10, 17942-17949.

13 S. Lu, M. Wang, F. Guo, J. Tu, A. Lv, Y. Chen and S. Jiao, *Chem. Eng. J.*, 2020, 389, 124370.